Journal of ELECTRONIC MATERIALS, Vol. 48, No. 12, 2019
https://doi.org/10.1007/s11664-019-07617-5

High-Performance Organic Field-Effect Transistors Fabricated with High-*k* Composite Polymer Gel Dielectrics

ARIF KÖSEMEN[1,2]

1.—Department of Physics, Muş Alparslan University, 49250 Muş, Turkey. 2.—e-mail: a.kosemen@alparslan.edu.tr

This study presents a composite gel-like dielectric material for organic field-effect transistors (OFET) applications. Poly(methyl methacrylate) (PMMA) gelled with propylene carbonate was used as gel dielectric material. Copper phthalocyanine was used as active layer in the OFET structures. In order to enhance the performance of the PMMA-gel dielectric material, silicium dioxide (SiO_2) was used as an additive material. Various ratios of SiO_2 were added to the gel dielectric and the effect of SiO_2 on the OFET performance was investigated. It was clearly observed that SiO_2 enhanced the performance and source-drain current of the fabricated OFETs. SiO_2 was added to the PMMA-gel with different doping ratios of 0%, 10%, 30%, 50% and 100% by using a solution-processing method. The dielectric properties of the PMMA-gel:SiO_2 composite materials were analyzed with impedance spectroscopy in terms of their effective capacitance (C), tangent factor ($\tan(\delta)$), phase angle and complex dielectric constant (ε' and ε''). The hole mobility of the OFETs was enhanced by 50% SiO_2 nanoparticles in PMMA-gel dielectric materials from 6.83×10^{-1} cm^2 V^{-1} s^{-1} to 4.66×10^{0} cm^2 V^{-1} s^{-1} (at $V_{DS} = -0.5$ V). The time-dependent I_{DS} curves were analyzed for OFETs fabricated with PMMA-gel:SiO_2 composite dielectric layers. It was found that all the devices worked stably under bias stress and gave fast responses for all gate voltages.

Key words: PMMA-gel gate dielectric materials, organic electronics, thin-film transistors, composite dielectrics

INTRODUCTION

Opto-electronic devices, in which conjugated polymers are used as active materials, have recently attracted considerable attention.[1–6] Among these devices, organic field-effect transistors (OFETs) are frequently investigated. There are many studies about the development of the performance of OFETs. However, a sufficient performance has not yet been achieved for commercial applications. The properties of gate dielectric materials for OFETs are very important to achieve low operation voltages, high mobility and high on/off ratios. In order to provide these properties, several methods have been investigated, such as combining high-*k* dielectric nano-particles with polymer dielectrics, high-k inorganic dielectrics, inorganic–organic bilayer dielectrics, self-assemble monolayer dielectrics and solid-state polymer electrolytes.[7–10] However, these methods are very difficult to implement and require complex technology.

High-performance, low-voltage-operating OFETs not only require gate insulators with good dielectric characteristics and high compatibility with the organic semiconductor but also facile, low-cost and reliable materials. Recently, there has been a significant interest in ion-gel electrolytes as dielectrics due to their large capacitance and facile fabrication in OFETs.[11] Frisbie et al. have successfully demonstrated a high-capacitance gate dielectric based on a solution-processable solid polymer electrolyte, poly(styrene-block-ethylene oxide-block-

(Received January 14, 2019; accepted September 4, 2019; published online September 12, 2019)

styrene) in an ionic liquid of 1-ethyl-3-methylimidazolium bis(trifluoromethylsulfonyl)imide. OFETs fabricated with the *p*-type polymer semiconductors poly(3-hexylthiophene) (P3HT), poly(3,3′-didodecylquaterthiophene) and poly(9,9′-dioctylfluorene-co-bithophene) [12] have yielded high I_{on} ($\sim 10^{-3}$–10^{-4} A) currents and low operating voltages (− 4.5 V). However, the slow polarization time associated with these electrolytes has been a significant disadvantage of this dielectric system in achieving fast transistor switching times.[13,14]

Poly(methylmethacrylate) (PMMA) with a solid thin-film form is a commonly used material for dielectrics in the OFET device structure due to its low dielectric constant and smooth and hydrophobic surface.[11,15] It has been shown in previous studies that the dipole moment of the solvent of the dielectric material is very important.[12] A stable and low-operating voltage (− 3 V) OFET with a solid thin-film form of PMMA was obtained dissolved in propylene carbonate (PC).[12] PC has also been used as a plasticizer material for the polymers.[16] The PC settles between the chains of the PMMA and keeps them further apart, thus reducing the forces of attraction between them and making the material more flexible. The gel has a reduced strength and stiffness compared to solid PMMA film because of the PC. PMMA-gel dielectric material has been used before in the structure of P3HT active layer-based OFETs and it was observed that operation voltages of the OFETs can go below 1 V.[17]

Composite materials composed of a mixture of organic and inorganic materials are used today in the development of new materials with superior properties for various applications.[18] Composite materials are used as a dielectric material for OFET applications.[19,20] When the dielectric film is obtained with an organic–inorganic mixture, the inorganic component improves the capacitive properties of the dielectric film, while the organic component of the mixture provides a uniform surface. However, use of this type of structure as the dielectric layer have some problems, such as surface roughness of the composite layers because of inorganic nanoparticles with the rough surface caused by the poor electrical parameters, such as high gate leakage current and low on/off current ratio.[21,22] These problems have been overcome by using another approach in which the organic and inorganic phases are more strongly bonded. There are many solid composite polymer-based studies using nano-structures such as SiO_2, TiO_2, ZrO_2 and Ta_2O_5.[23–26]

In this study, SiO_2nano-particles have been incorporated in PMMA-based gel dielectric materials with different ratios. The dielectric properties of the SiO_2-incorporated composite gel dielectrics were analyzed in detail and their effects on OFET performance were investigated. Less than 1 V operational voltage and high mobility values have been achieved by using a PMMA-gel:SiO_2 composite dielectric.

EXPERIMENTAL

Preparation of PMMA-gel:SiO_2 Composite Dielectrics

The materials used for preparation of the gel were purchased from Aldrich; acetonitrile (ACN), propylene carbonate (PC), PMMA (Mw ~24,400) and SiO_2 nano-particles (10–20 nm). The mixture was 70:20:10 in weight ratio, respectively. PMMA was dissolved in ACN at 150°C and PC was added in the mixture. Mixture was stirred until becoming gel viscosity. In order to incorporate the SiO_2 nanoparticles in the gel mixture before adding the PC, SiO_2 nanoparticles were added to the ACN solution. Weight ratios of SiO_2 nanoparticles to PMMA were arranged as 0%, 10%, 30%, 50%, and 100%.

Preparation of Gel Dielectric Capacitor and Dielectric Measurements

Polymer gel capacitor was constructed to investigate the impedance peculiarity of the proposed gel material with SiO_2 nano-particles. The capacitive properties of the PMMA-gel:SiO_2 gel dielectric were analyzed with a metal–insulator-metal (MIM) structure. The PMMA-gel dielectric material was sandwiched between Au-coated electrodes. Dielectric measurements of the MIM structure were made using a HP 4194A dielectric analyzer.

Preparation and Characterization of OFET Structure with Gel Dielectric

Sandwich-type OFET devices were fabricated using interdigitated Au source-drain electrodes on a glass substrate. The source-drain electrodes were photolithographically produced on the glass substrate. Source-drain electrodes are configured as interdigitated fingers with a channel length of 50 μm, and channel widths of the interdigitated electrodes are 60 mm. Figure 1 shows a schematic illustration of the OFET devices.

Cr (5 nm) was coated on the glass substrate and then Au (100 nm) was coated on the Cr layer using a thermally evaporation method. The Au electrode was etched with photolithography to produce an interdigitated source-drain electrode. CuPc (100 nm) was coated by thermal evaporation on the Au source-drain electrodes. CuPc thin films were annealed at 150°C for 15 min. PMMA-gel:SiO_2 composite dielectrics were sandwiched between the CuPc-coated source-drain electrodes and ITO electrodes were used as gate electrodes. The prepared PMMA-gel formulation was spread with a spatula over the semiconductor (CuPc). Teflon spacers (50 μm) were applied on either side of the interdigitated contact structure to fix the plasticized dielectric layer thickness at 50 μm. The output and

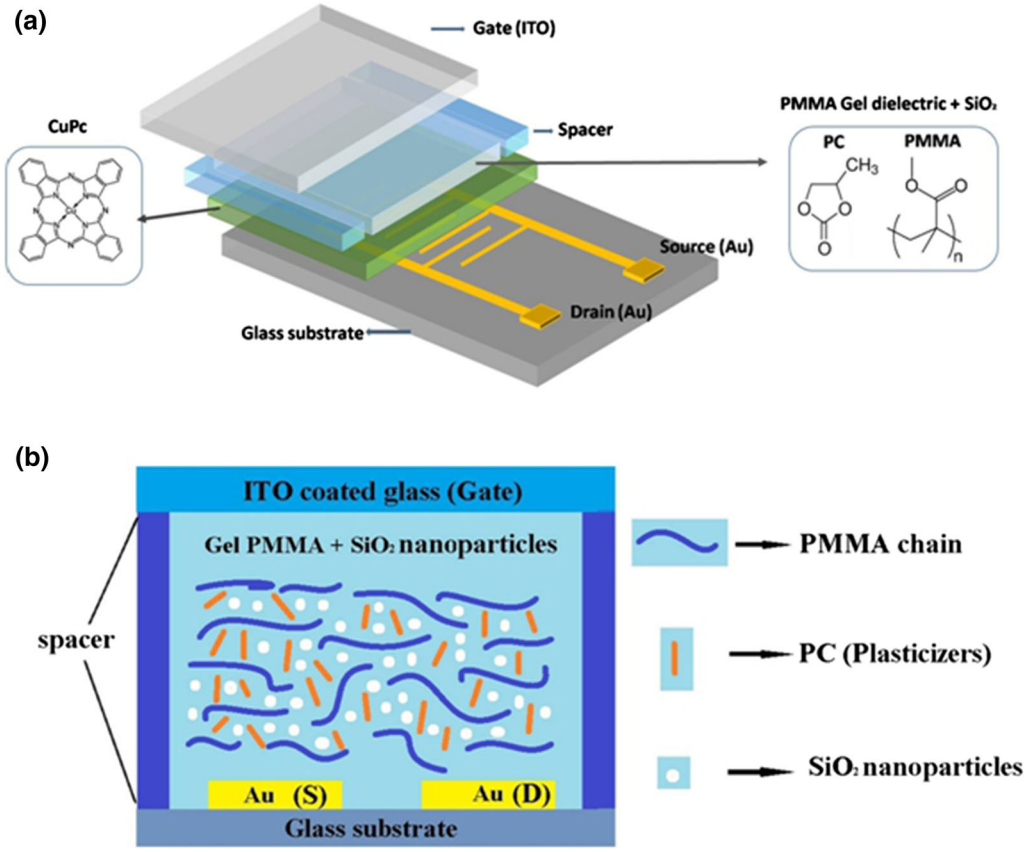

Fig. 1. (a) Schematic of assembled OFET devices. (b) Cross-sectional view of the OFET devices.

transfer characteristics of the OFETs were investigated via a Keithley 4200SCS.

RESULT AND DISCUSSION

The frequency dependence of the dielectric constants (imaginary and real), effective capacity, phase angle and tangent factor for PMMU-gel:SiO_2 composite dielectric materials have been investigated by impedance spectroscopy between 100 Hz to 10 MHz at room temperature. The frequency-dependent alteration of the effective capacity, $\tan(\delta)$ and phase angle for different doses of SiO_2 are given in Fig. 2. It is clearly seen from Fig. 2a that the capacitance decreasing rapidly and linearly from 10^2 Hz to 10^4 Hz and the decrease of the capacitance value slowed from 10^4 Hz to 10^7 Hz. High-capacitance values ($\sim$ 400 nF/cm^2 for pure, 10% and 30% SiO_2 added gel dielectric, $\sim$ 55 nF/cm^2 for 50% and 100% SiO_2 added polymer gel dielectrics at 100 Hz frequency) have occurred in the low-frequency region due to the predominance of the electrode polarization effect in the low-frequency region. In addition, the low capacitance value can be attributed to ion mobility in the high-frequency region. The reason why the PMMA-gel has a higher capacity value than PMMU thin film (10 nF/cm^2) at low frequency can be attributed to the high charge storage at the interface of the electrode and the PMMA-gel.[27–31] The capacity value of up to 30% of SiO_2 addition rate remained almost the same as pure PMMA-gel but, after this rate, it decreased rapidly for 50 and 100% doping rates. This can be attributed to the presence of SiO_2 nanoparticles in the gel medium disturbing the molecular orientation of the polymer chains. Because of the distortion of the polymer chains, dielectric anisotropy can be decreased. Since the dielectric constant ($\varepsilon' = \frac{C.d}{\varepsilon_0 A}$) is directly proportional to the capacity value, a decrease in the capacity value may also be observed. Dissipation factor (loss tangent, $\tan(\delta) = \frac{\varepsilon''}{\varepsilon'}$) can be considered as a characteristic part of the dielectric permittivity. Figure 2b gives the $\tan(\delta)$ as a function of frequency for SiO_2 added and unadded PMMA-gel composites. Relaxation peaks are clearly seen from the loss tangent spectra (Fig. 2b) and peak frequencies are named as critical frequencies (f_c). f_c values were observed to be shifted to lower frequency values by the increasing amount of SiO_2 in the PMMA-gel dielectric material (f_c = 800 Hz for without SiO_2 PMMA-gel, f_c = 120 Hz for 50% SiO_2-incorporated PMMA-gel). f_c is related to the relaxation times of the polymer chains in the gel medium described as $\tau_c = 1/2\pi f_c$. The relaxation time increases with the decrease in the f_c value according to the given formula. The increase in relaxation time may be due to the fact that the nanoparticles

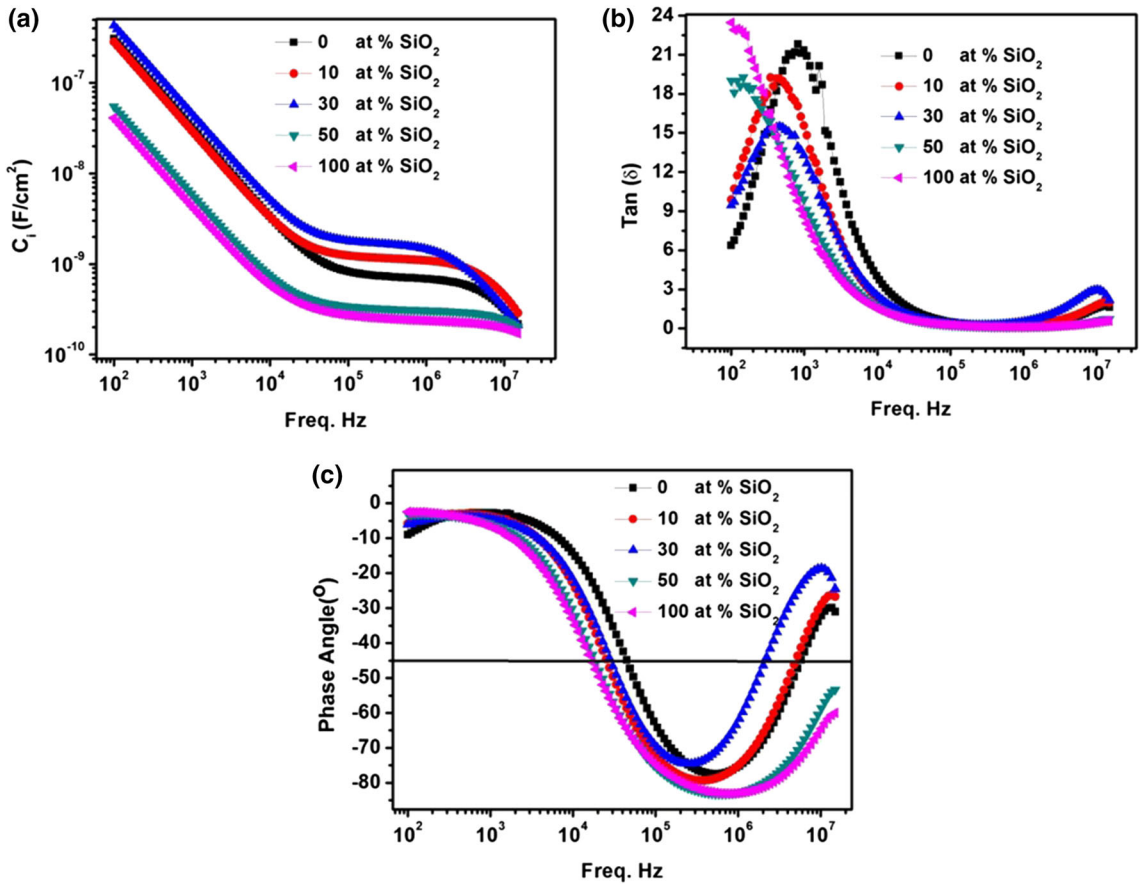

Fig. 2. Frequency evolution of the effective capacitance (a), tangent factor (tan(δ)) (b) and the phase angle (°) (c) for all the samples.

dispersed between the polymer chains reducing their ease of movement. Therefore, the f_c value may shift to lower frequencies. The frequency-dependent change in the phase angle is given in Fig. 2c. The phase angles of the unadded and SiO_2 nano-particle-added PMMA-gel dielectrics exhibit almost similar behavior. Frequency-dependent evaluation of the phase angle shows that the relaxation is capacitive when ($\theta < -45$) and resistive when ($\theta > -45$).[31] SiO_2-added and unadded PMMA-gel dielectric materials can be classified generally into two regions: when ($\theta > -45$) it is resistive in the smaller frequency region and when the frequency is greater than ($\theta < -45$) ,the gel becomes capacitive (Fig. 2c).It is clearly seen from the Fig. 2c that the frequency value returned from capacitive behavior to resistive behavior and shifted from 45 kHz to 17 kHz as the SiO_2 contribution increased.

The dependency of frequency for the real (ε') and imaginary (ε'') parts of the complex dielectric constant for PMMA-gel:SiO_2 composite dielectric materials are given in Fig. 3a and b, respectively. The ε' value of PMMA-gel dielectrics decreases with frequency from 10^2 Hz to 10^3 Hz and stays nearly constant from 10^3 Hz to 10^6 Hz. After 10^6 Hz, the frequency value ε' quickly decreases again (Fig. 3a). The frequency variation of ε'' decreases linearly to 10^5 Hz.

Frequency-dependent polarization characteristics for dielectric materials are related to their ionic polarization, space charge effect, dipolar polarization, atomic polarization and electronic polarization. The reason why PMMA-gel:SiO_2 materials have high ε' and ε'' values in low-frequency regions can be related to the electrode polarization effects. For the high-frequency regions ε' and ε'' values decreasing because the ions do not have sufficient time to orient in the field direction.[32–36] Significant changes were not observed in the ε' and ε'' values of the PMMA-gel:SiO_2 composite dielectric materials up to 30% SiO_2 added, but a noticeable decrease was observed for 50% and 100% SiO_2-added samples.

OFETs were fabricated in top gate–bottom contact configurations with unadded and SiO_2 nanoparticle-added PMMA-gel dielectrics. Transfer characteristics for all the samples are given in Fig. 4. The transistor parameters such as charge carrier mobility (μ), threshold voltage (V_{th}), and on/off ratio ($I_{on/off}$) are extracted from the transfer curves of the OFETs fabricated with unadded and SiO_2 nanoparticle-added PMMA-gel composite dielectrics. Field-effect mobilities can be determined from the saturation characteristics (μ_{sat}) of the OFET using the following equation:[37]

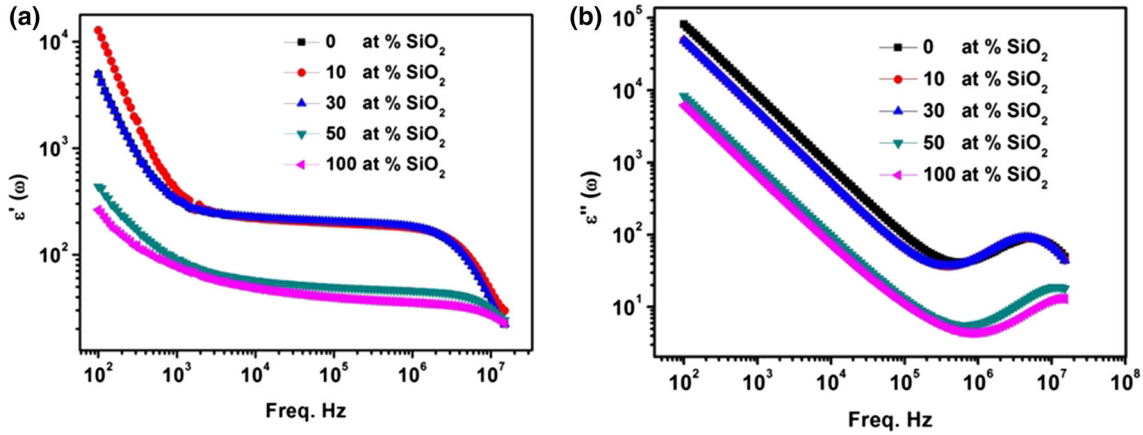

Fig. 3. Frequency evolution of the real part (a) and the imaginary part (b) of the complex dielectric constant for all the samples.

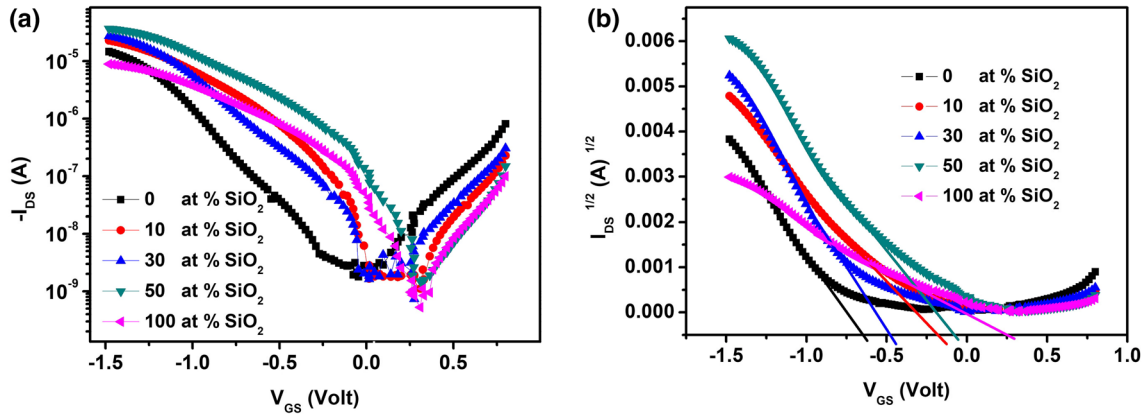

Fig. 4. Transfer characteristics curves of OFETs fabricated with pure and SiO_2 nanoparticle-added PMMA-gel dielectrics.

$$\mu_{\text{sat}} = \frac{2L}{WC_I}\left(\frac{\partial\left(I_{\text{ds,sat}}\right)^{1/2}}{\partial V_{\text{gs}}}\right)^2 \qquad (1)$$

where C_I is the capacitance of the unadded and SiO_2 nanoparticle-added PMMA-gel gate dielectrics taken at 100 Hz, W is the channel width (60 mm), L is the channel length (50 μm), V_{th} is the threshold voltage, and μ is the charge carrier mobility.

The transfer characteristics of OFETs fabricated with unadded and SiO_2 nanoparticle-added PMMA-gel dielectric materials were measured by sweeping the gate voltage from + 0.8 V to − 1.5 V. All devices exhibited p-type transistor behavior at a very low operation voltage < 1.5 V. The average hole mobility was calculated as 6.83×10^{-1} cm^2 V^{-1} s^{-1}for the unadded sample (at $V_{\text{DS}} = -0.5$ V). Highest mobility was calculated as 4.66×10^{0} cm^2 V^{-1} s^{-1} for the 50% SiO_2-added PMMA-gel dielectric OFET. These results indicate that the device performance can be enhanced by the addition in the PMMA-gel dielectric with inorganic nanoparticles despite the capacitive properties of the gel dielectric not being improved by the doping process. This can be attributed to the incorporation of SiO_2 nanoparticles in the PMMA-gel dielectric enhancing the stability of the gel dielectric and decreasing the interface traps thus making a better pathway for channel charge carriers. For the OFETs fabricated with solid dielectric materials, some studies have reported that mobility decreases with increasing the dielectric constant of the dielectric materials.[38,39] This situation can be explained by the polaronic self-localization of the accumulated charge carriers on the surface of the active layer occurring by the interaction of the active layer surface with the polarizable gate dielectrics.[40,41] For this reason, low mobility values have been revealed for the OFETs fabricated with larger dielectric constant gate dielectric materials. In this study, ε values of the PMMA-gel gate dielectric materials decreased by adding SiO_2 into the PMMA-gel dielectric material because of high μ value obtained with a high SiO_2 addition ratio. It is clearly observed from Fig. 4b that adding the SiO_2 affects the threshold voltages, i.e., the voltage value at which the current flow in the transistor channel starts, and shifted the more positive voltages with increased addition rates (Table I). This can be attributed to the changing of the dielectric/polymer interface with the addition of

Table I. Comparison of the performances of OFETs with a PMMA-gel:SiO_2 composite dielectric

Devices	V_{th}(V)	μ (cm^2/V s)	$I_{on/off}$
Pure PMMA-gel	− 0.6	6.83×10^{-1}	0.63×10^4
10% SiO_2:PMMA-gel	− 0.19	9.1×10^{-1}	0.85×10^4
30% SiO_2:PMMA-gel	− 0.48	8.18×10^{-1}	1.12×10^4
50% SiO_2:PMMA-gel	− 0.086	4.66×10^{-0}	1.38×10^4
100% SiO_2:PMMA-gel	+ 0.26	1.17×10^{-0}	0.37×10^4

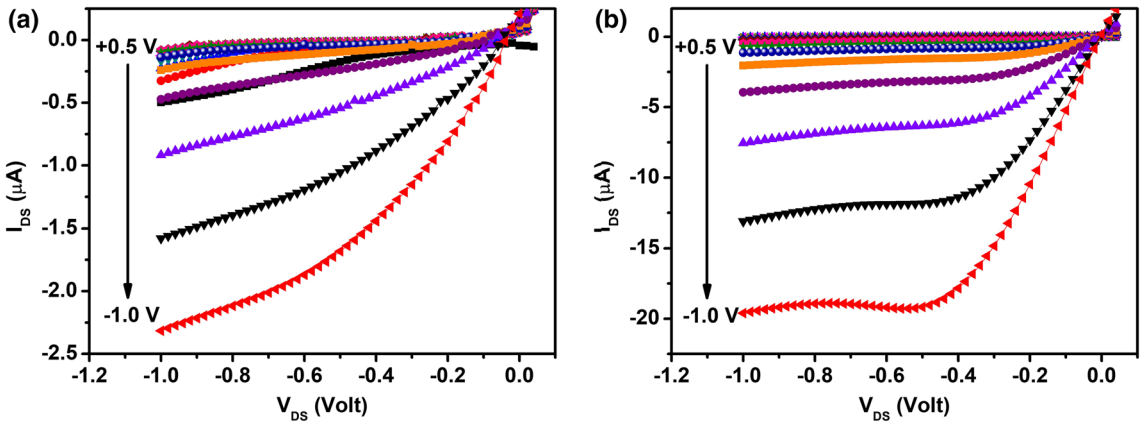

Fig. 5. Output characteristics curves of OFETs fabricated with (a) pure and (b) 50% SiO_2 nanoparticle-added PMMA-gel dielectrics.

the SiO_2 nanoparticles in the PMMA-gel dielectric.[37]

Figure 5 shows the output characteristics of the OFETs fabricated with pure PMMA-gel dielectric and 50% SiO_2-added PMMA gel dielectric layers. The output characteristics are found to be ideal with a good ohmic behavior at low source-drain voltages (V_{ds}) followed by saturation at higher V_{ds}. It can be clearly observed in Fig. 5 that the drain saturation current (I_D) of the 50% SiO_2 nanoparticle-added PMMA-gel dielectric OFET increases by 8 times compared to I_{DS} for the unadded PMMA-gel dielectirc OFET at V_{GS} = − 1 V and V_{DS} = − 1 V.

Figure 6 shows the time-dependent I_{DS} curves for OFETs fabricated with unadded and SiO_2 nanoparticle-added PMMA-gel dielectric layers. V_{DS} was kept constant at − 0.4 V during the measurements and V_{GS} was changed from 0 V, − 0.2 V, − 0.4 V, − 0.6 V, − 0.7 V and − 0.8 V with 20-s steps during 1000 s for all samples under the ambient conditions. It can be observed from Fig. 6 that all the devices work stably under bias stress and give fast responses for all gate voltages. It is clearly seen from Fig. 6 that SiO_2 addition in the PMMA-gel dielectric obviously affects the device performance. The I_{DS} value for OFETs is systematically increased with the addition of SiO_2 nanoparticles in the PMMA-gel dielectric up to 50% doping ratio, after which the I_{DS} value begin to decrease.

CONCLUSIONS

In this study, the effect of incorporating SiO_2 with different rates in PMMA-gel dielectrics on OFET performance was investigated and an efficient composite gel dielectric concept for using low operating voltage OFET applications has been suggested. Frequency-dependent dielectric properties [dielectric constant (imaginary and real), effective capacity, phase angle and tangent factor] of the pure and SiO_2 nanoparticle-added PMMA-gel dielectrics were analyzed with impedance spectroscopy between 100 Hz and 10 MHz frequency range at room temperature. Relatively high capacity values were reached for the unadded, 10% and 30% SiO_2 nanoparticle-added PMMA-gel dielectric materials of ~ 400 nF/cm^2, while the 50% and 100% contribution rate capacitance values decreased at approximately 55 nF/cm^2. High capacitance values occurred in the low-frequency region due to the predominance of the electrode polarization effect in the low-frequency region. The mobility of the OFETs was increased by the 50% SiO_2 addition in the PMMA-gel dielectric from 6.83×10^{-1} cm^2 V^{-1} s^{-1} to 4.66×10^0 cm^2 V^{-1} s^{-1} (at V_{DS} = − 0.5 V). It can be said that the addition of SiO_2 nanoparticles in the PMMA-gel dielectric obviously enhances the OFET performance. This can be attributed to the addition of the SiO_2

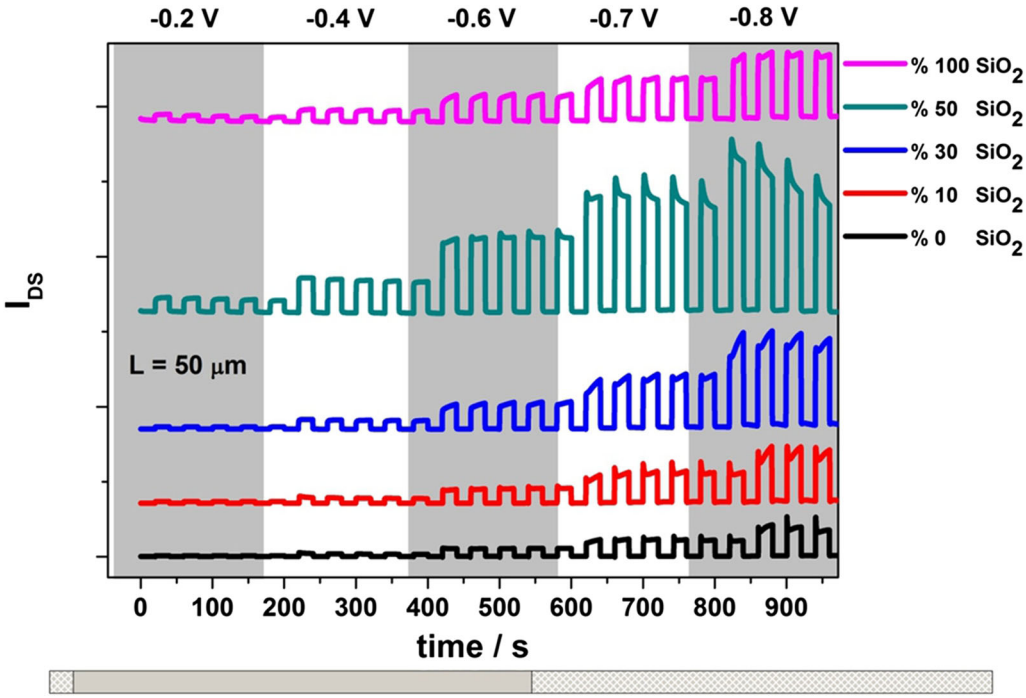

Fig. 6. Time-dependent measurement of OFETs fabricated with pure and SiO_2 nanoparticle-added PMMA-gel dielectrics.

nanoparticles in PMMA-gel dielectric enhancing the stability of the gel dielectric and decreasing the interface traps thus making a better pathway for channel charge carriers. This suggested material combination strategy may play an important role in the development of an attractive class of solution-processable gate dielectrics which will open up an entirely different branch of organic electronics. However, there are also considerable variables for further optimization of the performance, such as in the terms of choice of the high-k plasticizer and dielectric nanoparticles, dielectric polymer and its molecular weight, the concentration and process conditions.

REFERENCES

1. T.W. Kelley, P.F. Baude, C. Gerlach, D.E. Ender, D. Muyres, M.A. Haase, D.E. Vogel, and S.D. Theiss, *Chem. Mater.* 16, 4422 (2004).
2. H.E. Katz and J. Huang, *Annu. Rev. Mater. Res.* 39, 71 (2009).
3. M. Li, K. Gao, X. Wan, Q. Zhang, B. Kan, R. Xia, F. Liu, X. Yang, H. Feng, W. Ni, Y. Wang, J. Peng, H. Zhang, Z. Liang, H.-L. Yip, X. Peng, Y. Cao, and Y. Chen, *Nat. Photonics* 11, 85 (2017).
4. A. Korkmaz, A. Cetin, E. Kaya, and E. Erdoğan, *J. Polym. Res.* 25, 178 (2018).
5. K. Gao, J. Miao, L. Xiao, W. Deng, Y. Kan, T. Liang, C. Wang, F. Huang, J. Peng, Y. Cao, F. Liu, T.P. Russell, H. Wu, and X. Peng, *Adv. Mater.* 28, 4727 (2016).
6. K. Gao, S.B. Jo, X. Shi, L. Nian, M. Zhang, Y. Kan, F. Lin, B. Kan, B. Xu, Q. Rong, L. Shui, F. Liu, X. Peng, G. Zhou, Y. Cao, and A.K.-Y. Jen, *Adv. Mater.* 31, 1807842 (2019).
7. J. Veres, S. Ogier, G. Lloyd, and D. De Leeuw, *Chem. Mater.* 16, 4543 (2004).
8. B.L. Hu, K. Zhang, C. An, W. Pisula, and M. Baumgarten, *Org. Lett.* 19, 6300 (2017).
9. T. Lei, Y. Cao, Y. Fan, C.J. Liu, S.C. Yuan, and J. Pei, *J. Am. Chem. Soc.* 133, 6099 (2011).
10. M.E. Harb, S. Ebrahım, M. Solıman, and M. Shabana, *J. Electron. Mater.* 47, 353 (2018).
11. J.H. Choi, Y. Gu, K. Hong, W. Xie, C.D. Frisbie, and T.P. Lodge, *Appl. Mater. Interfaces* 6, 19275 (2014).
12. J.H. Cho, J. Lee, Y. Xia, B. Kim, Y. He, M.J. Renn, T.P. Lodge, and C.D. Frisbie, *Nat. Mater.* 7, 900–906 (2008).
13. M.J. Panzer and C.D. Frisbie, *Appl. Phys. Lett.* 88, 203504 (2006).
14. H. Shimotani, H. Asanuma, J. Takeya, and Y. Iwasa, *Appl. Phys. Lett.* 89, 203501 (2006).
15. W.L. Leong, N. Mathews, B. Tan, S. Vaidyanathan, F. Dötz, and S. Mhaisalkar, *J. Mater. Chem.* 21, 8971 (2011).
16. K. Hyung Lee, S. Zhang, T.P. Lodge, and C.D. Frisbie, *J. Phys. Chem. B* 115, 3315 (2011).
17. A. Kösemen, S.E. San, M. Okutan, Z. Doğruyol, A. Demir, Y. Yerli, B. Şengez, E. Başaran, and F. Yılmaz, *Microelectron. Eng.* 88, 17 (2011).
18. C.-T. Liu, W.-H. Lee and J.-F. Su, *Act. Passive Electron. Comp.* Article ID 2012, 7 (2012).
19. Y. Wang and H. Kim, *Org. Electron.* 13, 2997 (2012).
20. Y.-G. Ha, S. Jeong, J. Wu, M.-G. Kim, V.P. Dravid, A. Facchetti, and T.J. Marks, *J. Am. Chem. Soc.* 132, 17426 (2010).
21. C. Zhang, H. Wang, Z. Shi, Z. Cui, and D. Yan, *Org. Electron.* 13, 3302 (2012).
22. G.C. Choi and B.-S. Bae, *Synth. Met.* 159, 1288 (2009).
23. M.D. Morales-Acosta, C.G. Alvarado-Beltrán, M.A. Quevedo-López, B.E. Gnade, A. Mendoza-Galván, and R. Ramírez-Bon, *J. Non-Cryst. Solids* 362, 124 (2013).
24. A. Baharı and M. Shahbazı, *J. Electron. Mater.* 45, 1201 (2016).

25. D. Morales-Acosta, M. Quevedo-Lopez, B. Gnade, and R. Ramírez-Bon, *J. Sol-Gel Sci. Technol.* 58, 218 (2011).
26. B. Soltani and M. Babaeipour, *J. Mater. Sci. Mater. Electron.* 28, 4378 (2017).
27. R. Coskun, O. Yalçın, M. Okutan, and M. Öztürk, *J. Non-Cryst. Solids* 460, 153 (2017).
28. O. Yalçın, R. Coskun, M. Okutan, and M. Öztürk, *J. Phys. Chem. B* 117, 8931 (2013).
29. W.X. Yuan, *Solid State Sci.* 14, 330 (2012).
30. C. Arbizzani, M.C. Gallazzi, M. Mastragostino, M. Rossi, and F. Soavi, *Electrochem. Commun.* 3, 16 (2001).
31. O. Larsson, E. Said, M. Berggren, and X. Crispin, *Adv. Funct. Mater.* 19, 3334 (2009).
32. S. Ramesh, C.W. Liew, and A.K. Arof, *J. Non-Cryst. Solids* 357, 3654 (2011).
33. S.F. Mansour, *Egypt J. Solids* 28, 263 (2005).
34. G.B. Rao, P. Rajesh, and P. Ramasamy, *Mater. Res. Bull.* 60, 709 (2014).
35. S. Saha, A. Nandy, S.K. Pradhan, and A.K. Meikap, *Mater. Res. Bull.* 88, 272 (2017).
36. P. Maji, R.B. Choudhary, and M. Majhi, *Optik* 127, 4848 (2016).
37. Z. Alpaslan Kösemen, A. Kösemen, S. Öztürk, B. Canımkurbey, and Y. Yerli, *Mater. Sci. Semicond. Process.* 66, 207 (2017).
38. S. Ono, K. Miwa, S. Seki, and J. Takeya, *Appl. Phys. Lett.* 94, 063301 (2009).
39. A.F. Stassen, R.W.I. de Boer, N.N. Iosad, and A.F. Morpugo, *Appl. Phys. Lett.* 85, 3899 (2004).
40. S. Fratini, H. Xie, I.N. Hulea, S. Ciuchi, and A.F. Morpurgo, *New J. Phys.* 10, 033031 (2008).
41. S. Baldelli, *Acc. Chem. Res.* 41, 421 (2008).